

A preliminary study of the variation of phytoplankton absorption coefficients in the northern South China Sea

WU Jingyu^{1,2}, HONG Huasheng¹, SHANG Shaoling^{1*}, DAI Minhan¹, LEE Zhongping³,
LI Shaojing^{1,2}

¹ State Key Laboratory of Marine Environmental Science, Xiamen University, Xiamen 361005, China

² Department of Oceanography, Xiamen University, Xiamen 361005, China

³ Naval Research Lab, Code 7333, Stennis Space Center, MS 39529, USA

Received 29 September 2007; accepted 11 June 2009

Abstract

The temporal and spatial variabilities of phytoplankton absorption coefficients ($a_{ph}(\lambda)$) and their relationships with physical processes in the northern South China Sea were examined, based on in situ data collected from two cruise surveys during May 14 to 25, 2001 and November 2 to 21, 2002. Significant changes in the surface water in a_{ph} values and B/R ratios ($a_{ph}(440)/a_{ph}(675)$) were observed in May, which were caused by a phytoplankton bloom on the inner shelf stimulated by a large river plume due to heavy precipitation. This is consistent with the observed one order of magnitude elevation of chlorophyll *a* and a shift from a pico/nano dominated phytoplankton community to one dominated by micro-algae. Enhanced vertical mixing due to strengthened northeast monsoon in November has been observed to result in higher surface $a_{ph}(675)$ ($0.002\text{--}0.006\text{ m}^{-1}$ higher) and less pronounced subsurface maximum on the outer shelf/slope in November as compared with that in May. Measurements of a_{ph} and B/R ratios from three transects in November revealed a highest surface $a_{ph}(675)$ immediately outside the mouth of the Zhujiang (Pearl) River Estuary, whereas lower $a_{ph}(675)$ and higher B/R ratios were featured in the outer shelf/slope waters, demonstrating the respective influence of the Zhujiang River plume and the oligotrophic water of the South China Sea. The difference in spectral shapes of phytoplankton absorption (measured by B/R ratios and bathochromic shifts) on these three transects infers that picoprokaryotes are the major component of the phytoplankton community on the outer shelf/slope rather than on the inner shelf. A regional tuning of the phytoplankton absorption spectral model (Carder et al., 1999) was attempted, demonstrating a greater spatial variation than temporal variation in the lead parameter $a_0(\lambda)$. It was thus implicated that region-based parameterization of ocean color remote sensing algorithms in the northern South China Sea was mandatory.

Key words: phytoplankton absorption coefficient, variation, picoprokaryotes, parameterization, South China Sea

1 Introduction

The absorption and scattering coefficients of various water constituents determine the optical properties in the ocean (Preisendorfer, 1961). Among them, phytoplankton absorption coefficient (a_{ph}) is a critical component. Characterization of a_{ph} and its chlorophyll-specific counterpart (a_{ph}^*), as well as their sources and scales of variability, is important for a variety of applications such as remote sensing of chlorophyll *a* (chl *a*) concentration and primary production (e.g. Bidigare et al., 1987; Morel et al., 1996; Carder et al., 1999).

A general trend in oceanic waters is that a_{ph} at a specific wavelength (e. g. 440, 675 nm) is well correlated with chl *a* concentration, a major pigment in algal cells, while variation occurs in different regimes (Prieur and Sathyendranath, 1981; Carder et al., 1999; Cleveland, 1995; Lutz et al., 1996). A recent study in European coastal water reveals that the relationship between a_{ph} and chl *a* was overall similar to that previously established for open oceanic waters, although deviation occurred due to peculiar pigment composition and cell size (Babin et al., 2003). Similar results were also obtained in the Zhujiang River Estuary and the adjacent northeastern South China

Foundation item: The National Basic Research Program of China under contract Nos 2009CB421200, 2009CB421201; the National Natural Science Foundation of China under contract No.40821063; High-Tech R&D Program of China under contract Nos 2006AA09A302 and 2008AA09Z108.

*Corresponding author, E-mail: slshang@gmail.com

Sea (Cao et al., 2003; Xu et al., 2004). These studies generally support that a_{ph} should be a good indicator for changes of chl a and would be tightly associated with different water masses and physical dynamics.

Differences in phytoplankton absorption properties observed between and within species grown under various environmental conditions are ultimately governed by pigment composition and pigment package effects (Mitchell and Kiefer, 1988; Stramski and Morel, 1990; Sosik and Mitchell, 1991; Stuart et al., 1998; Lohrenz et al., 2003). For example, picoprokaryotes (cyanobacteria and marine prochlorophytes), the smallest phytoplankton group abundant in open ocean waters, were observed to have high a_{ph}^* (chlorophyll-specific absorption coefficient of phytoplankton) at 440 nm and blue/red (B/R) ratios (usually calculated as $a_{\text{ph}}(440)/a_{\text{ph}}(675)$) due to the low pigment package effects determined by their small cell size and the high zeaxanthin or divinyl chl b concentration (Kana et al., 1988; Moore et al., 1995). Divinyl chl a/b contained in marine prochlorophytes show a ca. 8 nm bathochromic shift of absorption maximum compared to the normal chl a/b (Chisholm et al., 1988). Thus, variation of a_{ph} may be reflective of the variation in chl a as well as the phytoplankton community structure, which suggests an alternative optical approach to phytoplankton study especially when HPLC (high performance liquid chromatography) or flow cytometry data are not available (Moore et al., 1995). Most importantly, since a_{ph} can be remotely estimated, its potential application could be powerful.

Development of algorithms to retrieve absorption coefficients remotely, from empirical to full-spectral optimization, has been underway (e.g. Lee et al., 1998; Carder et al., 1999; Lee et al., 2002), and the retrieval accuracy of semi-analytical algorithms is often better than that of empirical algorithms (Bukata et al., 1995; IOCCG, 2000). However, the performance of these algorithms relies on accurate parameterization in the spectral models for the absorption coefficients of phytoplankton pigments and other light absorbing constituents. The spectral models for phytoplankton absorption are subject to spatial and temporal variation due to changing pigment composition and package effects. As a consequence, regional in situ studies of the variability of phytoplankton absorption properties are fundamental in order to parameterize the spectral models towards algorithms for remote sensing applications.

The South China Sea (SCS) is one of the major

marginal seas. The Zhujiang River discharges into its northeast, through which the SCS receives freshwater as well as nutrients and pollutants from one of the most industrialized regions of China. Climatic variations in the atmosphere and the upper ocean of the SCS are primarily controlled by the East Asian monsoon, which follows closely the variations in the equatorial Pacific (Liu et al., 2002). Although it is basically an important low latitude marginal sea, its biogeochemistry has received relatively little attention. Recent arguments emerged towards a role of CO₂ source the SCS played (Zhai et al., 2005; Cai and Dai, 2004). Spatial and temporal patterns of phytoplankton are thus essential to understand the carbonate system. However, knowledge on phytoplankton, including chl a , taxonomy, primary production and the optical properties, is extremely limited, especially in the northern SCS (NSCS) adjacent to the Zhujiang River Estuary (ZRE). There are a couple of reports found but the spatial and temporal changes are rarely discussed (Huang et al., 2002; Cao et al., 2003, 2005; Ning et al., 2003, 2004; Zhu et al., 2003; Lee Chen, 2005; Wang et al., 2005, 2007).

Based on two cruise surveys conducted in the northern South China Sea in May 2001 and November 2002, this paper attempts to utilize a_{ph} as an alternative parameter for chl a and taxonomy and thus aims to examine the variation of phytoplankton absorption coefficients associated with hydrodynamics, in particular the changes in response to a plume event, and changes between a southwest monsoon season in May and a northeast monsoon season in November. Change of the a_{ph} spectral model parameterization is also examined to provide helpful information for local semi-analytical remote sensing algorithm.

2 Material and methods

The NSCS was surveyed during two cruises (May 14 to 25, 2001 and November 2 to 21, 2002) on board R/V *YanpingII*. Figure 1 shows the stations for CTD surveys and absorption sampling. The 2001 cruise involved one transect (Transect A, hereafter T-A), starting from the vicinity of the ZRE to the southeast to Dongsha Island, and crossing the shelf to the slope. The 2002 cruise had two more transects: Transect B (hereafter T-B) parallel to and to the east of T-A, and Transect C (hereafter T-C) located outside the ZRE, along the coast. Following Zhai et al. (2005), T-A can be divided into two zones, inner shelf with water

depths shallower than 100 m and within a range of ca. 75–130 km from the coast (Stas 6C, 6 and 5A); and outer shelf/slope with water depths of 100–1 000 m (Stas 5, 4A, 2, 4, 3 and 3A).

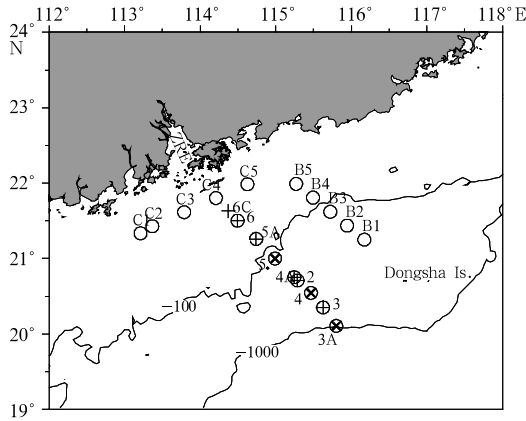


Fig.1. CTD and sampling stations in the northern South China Sea. +: CTD and sampling stations in May 2001; ×: stations only for CTD in May 2001; ○: CTD and sampling stations in November 2002; ZRE: the Zhujiang River Estuary; Dongsha Is.: Dongsha Island.

Our May 2001 cruise was divided into two legs. The first cruise leg was between May 14–19, and the second was during May 24–25. Stations 6 & 2 were sampled in both cruise legs for absorption coefficients (the second sampling is annotated as Sta. 6' and Sta. 2', respectively).

Our sample collection and measurements strictly followed the Ocean Optics Protocols Version 2.0, distributed by NASA (Mitchell et al., 2000). Briefly, water samples were collected with 1.7 L Niskin bottles mounted on a rosette equipped with a SBE19 CTD which provides temperature and salinity data. Samples were then filtered onto a 25 mm 0.7 μm glass fiber filter (Whatman GF/F) under low vacuum (<17 kPa). Sample filters were put into tissue capsules (Fisher HistoprepTM) and then stored in liquid nitrogen for subsequent laboratory analysis at Xiamen University.

Absorption was measured on a dual-beam Varian Cary-100 spectrophotometer equipped with an integrating sphere. Sample filters were first scanned from 250 to 800 nm relative to a blank filter saturated with 0.2 μm filtered seawater to obtain the total particulate absorbance spectra (OD_p). After pigment extraction with methanol, sample filters were measured again to obtain the absorbance spectra of the nonalgal particles (OD_d). $OD_p(440)$ and $OD_d(440)$ were all less than 0.4

absorbance.

Absorption coefficients of total particles (a_p) and nonalgal particles (a_d) were calculated as:

$$a(\lambda) = 2.303 \times [OD(\lambda) - OD_{\text{null}}] \times \frac{A}{V\beta},$$

where A is the area of the sample filter with concentrated particles, V is the volume of water filtered and β is a parameter to correct for the pathlength amplification effect due to multiple scattering. Many relationships exist regarding the β parameter (Mitchell et al., 2000), and we used the expression developed by Cleveland and Weidemann (1993) as the measurement geometry relatively similar to our setup. OD_{null} is the average of the OD between 790 and 800 nm since it has been found that all aquatic particles generally show negligible absorption in the near infrared. Phytoplankton absorption coefficients (a_{ph}) were then calculated as the difference between a_p and a_d .

Since a_{ph} at 675 nm is mainly associated with chl a and is less influenced by pigment package effects, hereafter we choose it to indicate the variation of a_{ph} . In addition, the absorption of water samples from depths >150 m was found too weak to be detected, therefore only data for the upper 150 m of water are presented.

3 Results and discussion

3.1 Variations of a_{ph} magnitude and spectral shapes

3.1.1 Short term variation in May 2001

The outburst of the SCS summer monsoon normally occurs in mid-May, leading to a rainy season (Qian et al., 2002). This was also the case in May 2001. Heavy precipitation appeared on May 1, May 7–9, May 17–18, and May 21–22, recorded at both Baiyun (Guangzhou) and Hong Kong weather observatories as described in a parallel study (Dai et al., 2008). Accumulation of this precipitation caused a river plume extending to the region near Sta. 6 as evidenced by low salinity between May 24 and 25 (Fig. 2). Surface water salinity sharply dropped from 34.0 to \sim 26.5 at Sta. 6. The plume, which apparently diminished at Sta. 5A, brought a significant amount of nutrients into the region shoreward of Sta. 5A, resulting in a phytoplankton bloom, as revealed by a parallel study on the carbonate system in this region (Dai et al., 2008).

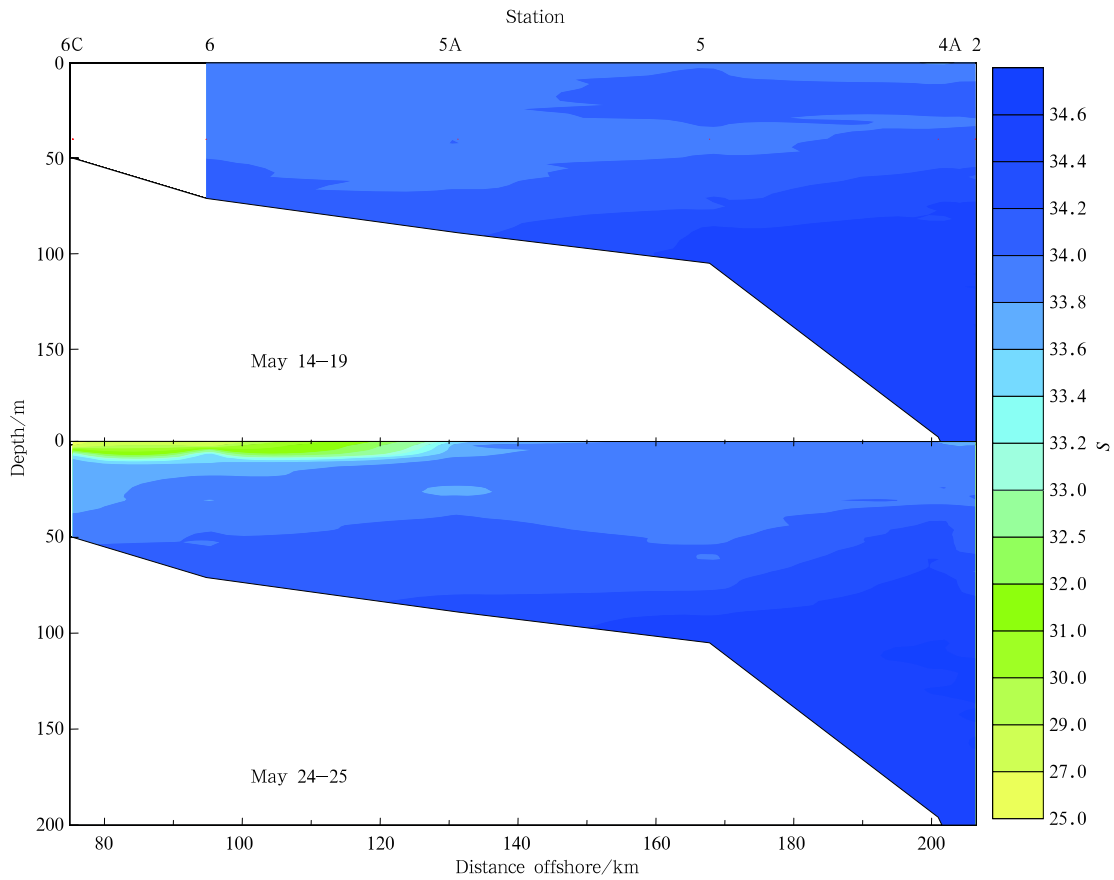


Fig.2. Changes of salinity between the two cruise legs in May 2001.

Correspondingly, the absorption properties experienced significant changes during this period of observation. Figure 3 shows vertical profiles of $a_{ph}(675)$ observed on T-A in May 2001. During the first cruise leg between May 15 and 19, the surface $a_{ph}(675)$ varied from 0.002 m^{-1} at Sta. 6 to 0.004 m^{-1} at Sta. 5A (~37 km apart) on the inner shelf, and no significant changes were found between the inner shelf and the outer shelf/slope. A subsurface maximum in

$a_{ph}(675)$ existed both on the inner shelf and the outer shelf/slope, with value varying between $0.015\text{--}0.019\text{ m}^{-1}$. During the second cruise leg between May 24–25, however, the horizontal gradient of $a_{ph}(675)$ increased substantially. On the inner shelf, the surface $a_{ph}(675)$ became one order of magnitude higher than that on the outer shelf/slope. $a_{ph}(675)$ as high as 0.050 m^{-1} occurred at Sta. 6. This was equivalent to an increase of chl *a* from 0.1 to 2.6 mg/m^3 using the model of

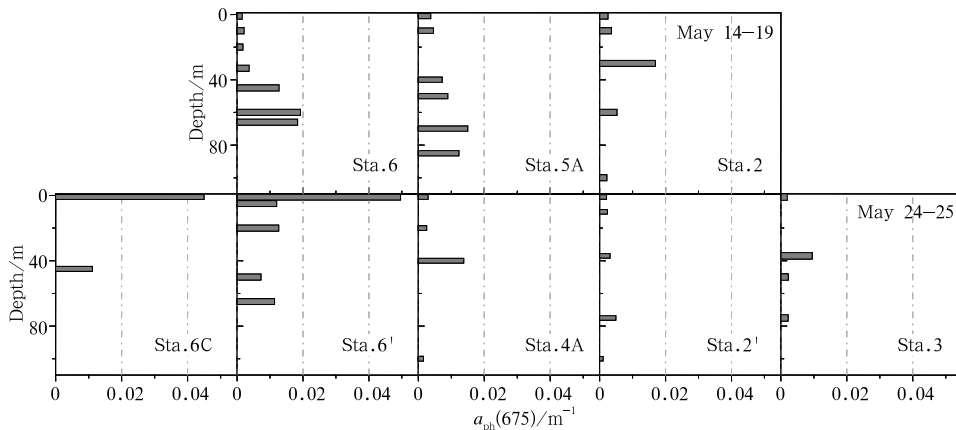


Fig.3. Vertical distribution of $a_{ph}(675)$ during the two cruise legs in May 2001.

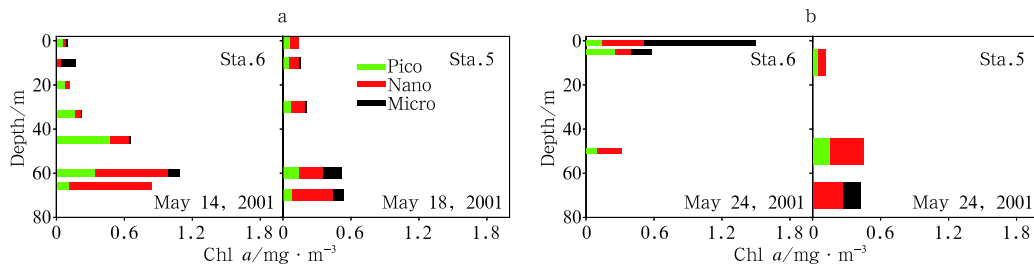


Fig. 4. Changes of size-fractionated chl *a* at stations 6 and 5 between the two cruise legs in May 2001, cited from Dai et al. (2008).

Carder et al. (1999) ($[\text{chl } a] = 56.8 \times [a_{\text{ph}}(675)]^{1.03}$), which was consistent with the observed one order of magnitude elevation of chl *a* as reported by Dai et al. (2008) (Fig. 4). The occurrence of a phytoplankton bloom around Sta. 6 was thus evident. In contrast, the outer shelf/slope maintained a low surface $a_{\text{ph}}(675)$ around 0.002 m^{-1} and a subsurface/deep maximum varying between $0.005\text{--}0.014 \text{ m}^{-1}$. For the two stations we revisited, significant changes were solely found at Sta. 6, where surface $a_{\text{ph}}(675)$ increased from 0.002 to 0.050 m^{-1} .

B/R ratios ($a_{\text{ph}}(440)/a_{\text{ph}}(675)$) on the inner shelf also showed significant changes (Table 1). During the first cruise leg, the surface B/R ratios, both on the inner shelf and on the outer shelf/slope, were greater than 3.0. Typical eukaryotic phytoplankton studied in the laboratory has not been observed with peak B/R ratios in excess of 2.5 (Cleveland et al., 1989), while picoprokaryotes can exhibit B/R ratios much greater than that (Stramski and Morel, 1990; Partensky et al., 1993; Moore et al., 1995). This implies the predominance of picoprokaryotes in the phytoplankton community during the first survey. However, during the second leg, surface B/R ratio at Sta. 6 dropped from 3.9 to 2.5, suggesting a decrease in the proportion of picoprokaryotes in the phytoplankton community. This can be confirmed by the finding in a parallel carbonate system study, which demonstrates that the phytoplankton community structure in terms of size-fractionated chl *a* significantly shifted from a pico/nano-phytoplankton dominated community to a structure dominated by micro-algae in surface water at Sta. 6 during the second cruise leg (Fig. 4; Dai et al., 2008). Moreover, the shape of the a_{ph} spectrum changed substantially in the shorter wavelengths (Fig. 5). Stronger absorptions were found at 636 and 485 nm, suggesting abundance of chl *c* and fucoxanthin, typically contained in diatoms (Bidigare et al., 1990). The absorption maximum in the blue region shifted

from 440 to 432 and 410 nm, indicating increasing levels of phaeopigments (Lorenzen and Downs, 1986). It thus implies that a diatom bloom at its late stage occurred around Sta. 6 when the second cruise leg took place. It should be noted that similar features in the a_{ph} spectra were observed at Sta. 6C (shoreward of Sta. 6, Fig. 5) with a B/R ratio as low as 2.1. On the outer shelf/slope, however, B/R ratios remained greater than 3.0 throughout the cruise.

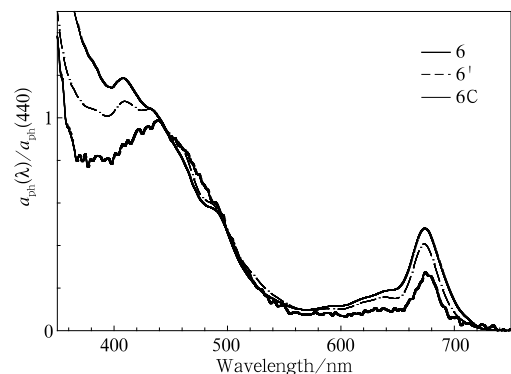


Fig. 5. Surface a_{ph} normalized at 440 nm at Sta. 6 and Sta. 6C. Sta. 6C was sampled during the second cruise leg when Sta. 6 was revisited (annotated as Sta. 6').

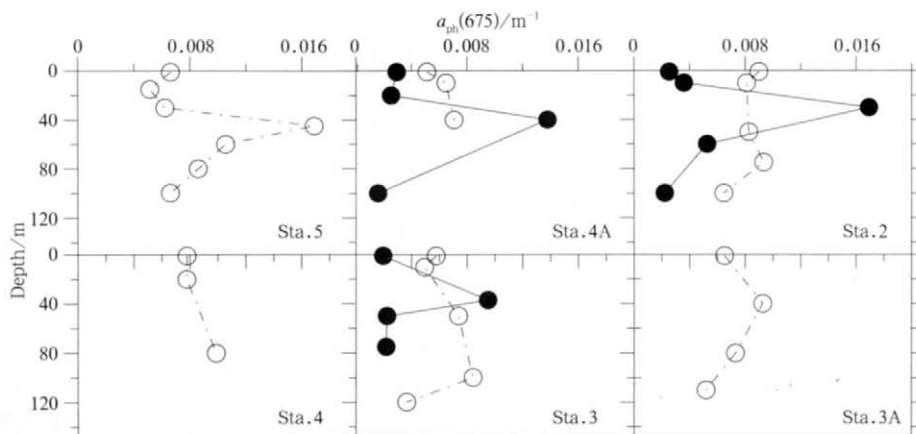
3.1.2 Variation in the outer shelf on Transect A between May and November

The inner shelf water on T-A was clearly subject to significant short term variations in May (a high flow season of the ZRE). Comparisons of a_{ph} between May and November, southwest and northeast monsoon seasons, will thus focus on the outer shelf/slope of T-A.

Both the surface value and the vertical structure of $a_{\text{ph}}(675)$ on the outer shelf/slope of T-A in November 2002 differed from that in May 2001 (Fig. 6). For example, surface $a_{\text{ph}}(675)$ along T-A varied from 0.005 to 0.009 m^{-1} in November, higher by $0.002\text{--}0.006 \text{ m}^{-1}$ than those observed at the same stations in May 2001.

Table 1. B/R ratios ($a_{ph}(440)/a_{ph}(675)$) in the Northern South China Sea in May 2001 and November 2002

2001-5			2002-11					
station	depth/m	B/R ratio	station	depth/m	B/R ratio	station	depth/m	B/R ratio
3	1	3.4	3A	1	3.4	C1	1	2.6
3	37	2.6	3A	40	2.9	C1	5	2.9
3	50	2.6	3A	80	2.3	C1	39	2.2
3	75	3.8	3A	110	2.4	C2	1	2.8
2	1	3.4	3	1	3.2	C2	10	2.6
2	10	3.1	3	10	3.5	C2	35	2.1
2	30	2.3	3	50	2.8	C3	1	2.1
2	60	2.5	3	100	2.1	C3	7	2.3
2	100	3.4	3	120	2.3	C3	31	2.2
4A	1	3.6	4	1	3.1	C4	1	2.3
4A	20	3.8	4	20	3.0	C4	10	2.3
4A	40	2.3	4	80	2.3	C4	20	2.3
4A	100	3.6	2	1	2.6	C4	42	1.9
5A	1	3.3	2	10	2.6	C5	1	2.0
5A	10	3.1	2	50	2.7	C5	40	2.3
5A	40	2.7	2	75	2.3	B1	1	3.7
5A	50	2.6	2	100	2.5	B1	20	3.4
5A	70	2.3	4A	1	3.1	B1	40	2.5
5A	85	2.5	4A	10	2.9	B1	70	2.5
6	1	3.9	4A	40	2.9	B1	120	2.7
6	10	3.4	5	1	2.7	B2	1	3.5
6	20	3.9	5	15	3.1	B2	20	2.2
6	33	3.2	5	30	3.2	B2	50	2.9
6	45	2.6	5	45	2.5	B2	80	3.6
6	60	2.5	5	60	2.0	B2	100	2.4
6	66	2.4	5	80	3.0	B2	140	2.2
2'	1	3.2	5	100	2.9	B3	1	3.5
2'	10	3.4	5A	1	2.4	B3	10	3.3
2'	37	3.2	5A	5	2.5	B3	60	2.5
2'	75	2.3	5A	10	2.4	B3	80	2.4
2'	100	2.7	5A	25	2.2	B3	100	3.3
6'	1	2.5	5A	50	2.3	B4	1	3.5
6'	5	2.6	5A	84	2.4	B4	20	3.0
6'	20	2.6	6	1	2.5	B4	50	2.2
6'	50	2.4	6	15	2.4	B4	80	3.8
6'	65	2.5	6	25	2.6	B5	1	3.4
6C	1	2.1	6	35	2.6	B5	60	2.4
6C	45	2.3	6	65	2.3			

**Fig.6.** Vertical distribution of $a_{ph}(675)$ on the outer shelf/slope of transect A. Observations in May 2001 and November 2002 are represented with bold and open circles respectively.

Although subsurface maxima also existed in November, they were far less prominent than those in May. The differences between the subsurface maxima and the surface values were typically less than 0.003 m^{-1} in November for most stations, whereas in May they were higher by at least a factor of two as compared

to the November values. Average B/R ratios on the outer shelf of T-A were slightly higher in May than in November (Table 2), although they were generally greater than 3.0 in the upper water in both seasons. It might suggest that picococaryotes contributed more to the total phytoplankton biomass in May than in

Table 2. Parameters of the phytoplankton absorption spectral model

Wavelength/mm	Parameters	May-2001 T-A	Nov.-2002 T-A	Nov.-2002 T-B	Nov.-2002 T-C	Carder et al. (1999)
412	a_0	2.00	1.85	1.94	1.53	2.2
	a_1	0.45	0.29	0.55	-0.21	0.75
	a_2	-0.5	-0.5	-0.5	-0.5	-0.5
	a_3	0.011 2	0.011 2	0.011 2	0.011 2	0.011 2
	R^2	0.96	0.90	0.89	0.78	\
443	a_0	2.39	2.38	2.53	1.96	3.59
	a_1	0.49	0.26	0.29	0.26	0.8
	a_2	-0.5	-0.5	-0.5	-0.5	-0.5
	a_3	0.011 2	0.011 2	0.011 2	0.011 2	0.011 2
	R^2	0.99	0.94	0.92	0.66	\
488	a_0	1.73	1.62	1.78	1.39	2.27
	a_1	0.36	0.27	0.35	0.27	0.59
	a_2	-0.5	-0.5	-0.5	-0.5	-0.5
	a_3	0.011 2	0.011 2	0.011 2	0.011 2	0.011 2
	R^2	0.99	0.97	0.97	0.77	\
510	a_0	1.02	0.89	0.96	0.86	1.4
	a_1	0.33	0.32	0.51	-0.43	0.35
	a_2	-0.5	-0.5	-0.5	-0.5	-0.5
	a_3	0.011 2	0.011 2	0.011 2	0.011 2	0.011 2
	R^2	0.97	0.92	0.93	0.94	\
551	a_0	0.38	0.30	0.34	0.33	0.42
	a_1	-0.66	0.06	0.39	-1.88	-0.22
	a_2	-0.5	-0.5	-0.5	-0.5	-0.5
	a_3	0.011 2	0.011 2	0.011 2	0.011 2	0.011 2
	R^2	0.87	0.68	0.64	0.87	\

November.

On the average, the transition from the north-east to southwest monsoon in the SCS occurs in May and the transition from the southwest to the north-east occurs in October (Lau et al., 1998). Figure 7 displays the monthly mean distribution of QuikSCAT wind stress in the region under study in May 2001 and November 2002. The maximum northeasterly wind stress in November 2002 could be up to 0.25 N/m^2 . The wind stress in May 2001 was much smaller (mostly $<0.1 \text{ N/m}^2$) and variable in direction. The effect of wind forcing superimposed on surface cooling convective overturn in the northeast monsoon season would lead to enhanced vertical mixing, resulting in the deepening of mixed layer depth (MLD). The deepening of MLD in the region of interest in November 2002 as compared to that in May 2001 was obvious (Fig. 8). Except for Sta. 5, which was located at 100 m isobath,

MLD on the outer shelf/slope of T-A varied between 60–100 m in November, while it was less than 20 m in May. This indicates that the nutrients in the upper nutricline are more readily for primary production, leading to elevated chl *a*, as observed at a SCS time series station (SEATS) located in the NSCS (Tseng, et al., 2005). Consequently, it is reasonable to find high surface values and less prominent subsurface maxima for $a_{\text{ph}}(675)$ in November, accompanied by a decrease and less prominent vertical variability in B/R ratios. However, it should be noted that B/R ratios may be partly a result of photoacclimation. Seasonal variation in phytoplankton community structure is difficult to deduce from such a difference since there is greater solar irradiance in May.

3.1.3 Spatial variation in November 2002

The survey of November 2002 covered broader regions, including T-B and T-C, in addition to T-A.

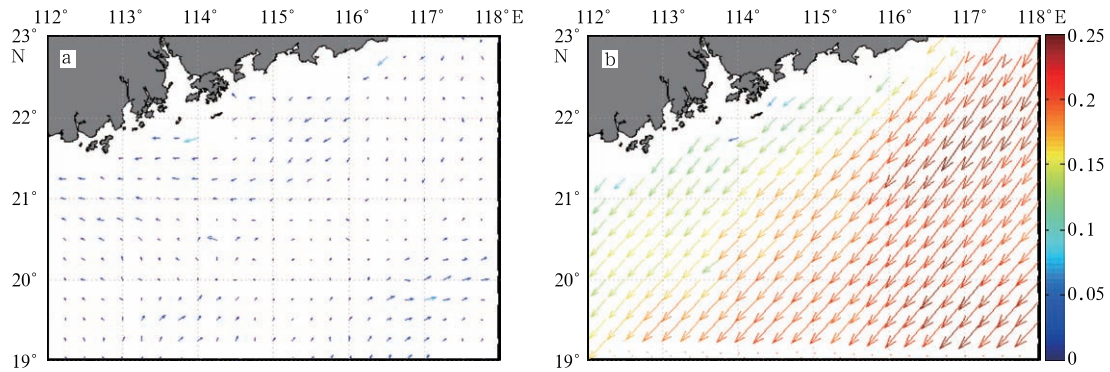


Fig.7. Monthly mean wind stress as observed by QuikSCAT during May 2001 (a) and November 2002 (b). The unit is N/m^2 .

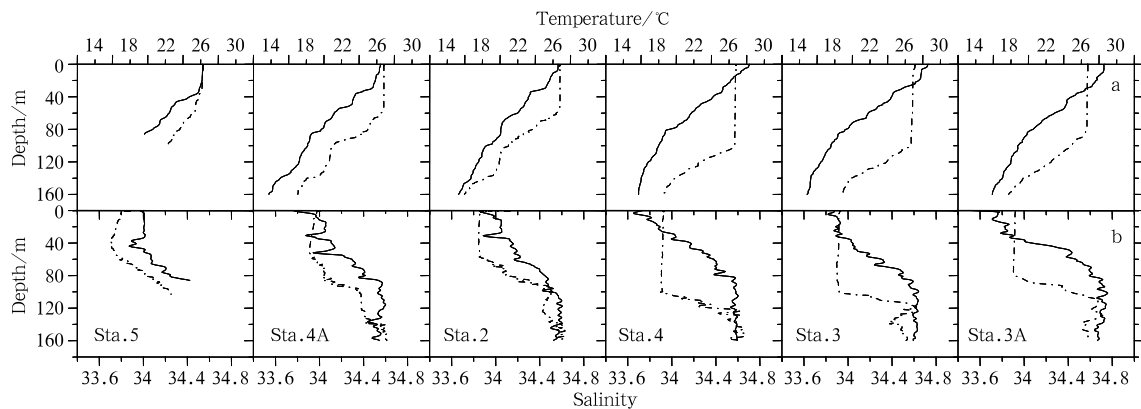


Fig.8. Temperature (a) and salinity (b) profiles on the outer shelf/slope of transect A. The solid and dash lines represent observations in May 2001 and November 2002, respectively.

Figure 9 displays their different hydrological properties. T-C was within ~ 50 km distance from the coast, highly impacted by Yuedong Coastal Water. This water mass is low in salinity but rich in nutrients, thus maintains a relatively high level of chl a and primary productivity (Li and Su, 2001). T-B and T-A were on the shelf. T-B was located east of the ZRE. Since the Zhujiang River plume went southwestward under the forcing of the northeast monsoon in November (Su, 2004), T-B was beyond the impact of the Zhujiang River plume. T-A, on the contrary, was right outside the ZRE. Nutrient loadings from the river plume to T-A was thus expected. On the other hand, it was suggested that vertical turbulence might have been reinforced on T-A due to the input of the Zhujiang River plume (Mann and Lazier, 1996), leading to a deeper MLD on T-A than on T-B (Fig. 9). This implies that nutrients might be more available for phytoplankton growth in the upper layer on T-A.

Corresponding to the different physical regimes, a clear spatial pattern of $a_{ph}(675)$ appeared. As Fig. 10

shows, surface $a_{ph}(675)$ was much higher on T-C than that on T-B and T-A except at Sta. 5A. It ranged between 0.010 – $0.018 m^{-1}$ on T-C, corresponding to a range of chl a between 0.49 – $0.91 mg/m^3$ according to the algorithm of Carder et al. (1999). The highest value occurred at Sta. C4, which was located facing and closest to the ZRE, demonstrating that the Zhujiang River plume in this low flow season could still be influential to the area around $21.8^\circ N$ (see Fig. 1 for the location). There was no distinct subsurface/deep maximum in $a_{ph}(675)$ on T-C, although $a_{ph}(675)$ was slightly higher in deeper water than at the surface.

Surface $a_{ph}(675)$ of T-B was relatively low compared to that of T-A, either on the inner shelf or on the outer shelf/slope. It was nearly homogenous, staying around $0.005 m^{-1}$ over the entire T-B. In contrast, it had a greater horizontal gradient along T-A, varying between a minimum of $0.005 m^{-1}$ on the outer shelf/slope and a maximum of $0.015 m^{-1}$ on the inner shelf. Vertical structures of $a_{ph}(675)$ were also different. A prominent subsurface $a_{ph}(675)$ maximum was

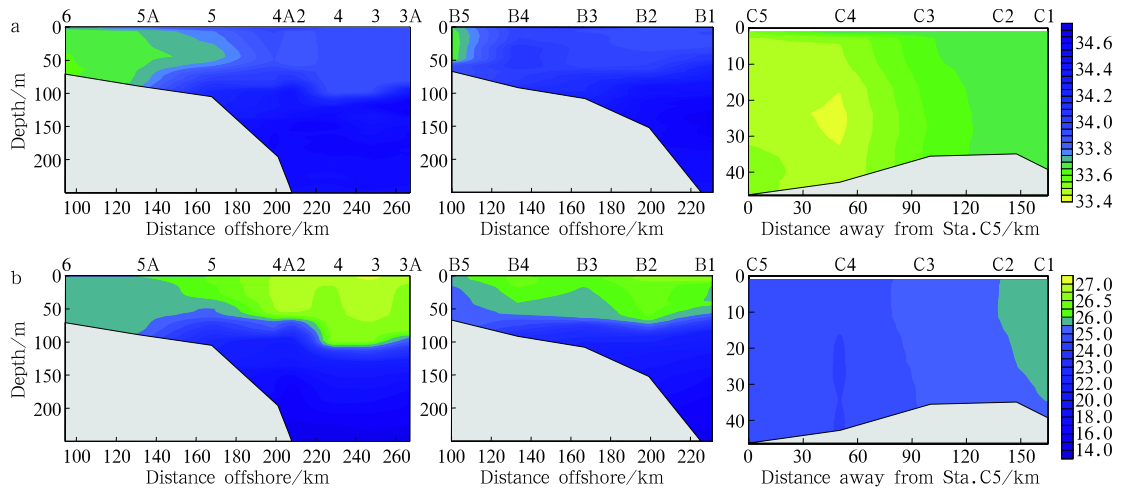


Fig.9. Salinity (a) and temperature ($^{\circ}\text{C}$) (b) distribution on Transect-A, B and C (from left to right) in November 2002.

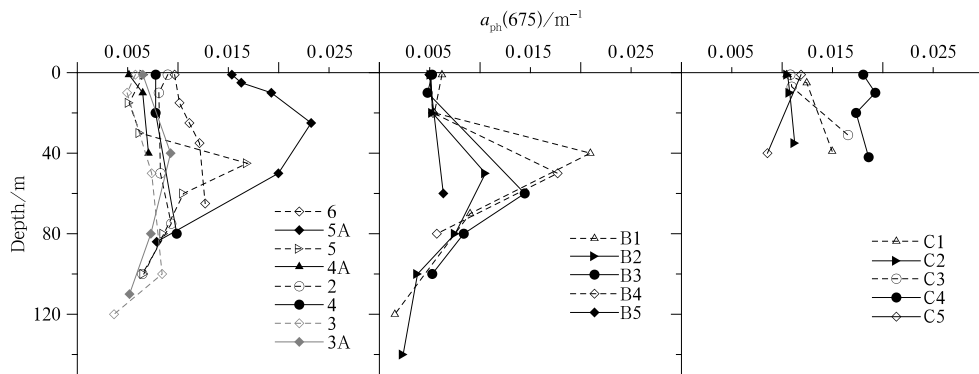


Fig.10. Vertical profiles of $a_{\text{ph}}(675)$ in November 2002 on T-A, T-B and T-C.

present on T-B, with a maximum level of 0.021 m^{-1} , especially on the outer shelf/slope. For T-A, although a subsurface $a_{\text{ph}}(675)$ maximum was visible, the values were lower. These variations of $a_{\text{ph}}(675)$ between two shelf transects, T-A and T-B, clearly indicate that the Zhujiang River plume affected the inner shelf of T-A by supplying more nutrients for phytoplankton growth, either through direct input or by enhancing vertical mixing.

B/R ratios also changed among the three transects (Table 1). Generally, T-C had the lowest value (<2.5 for most stations) and T-B had the highest (>2.5 for most stations) (Table 1). On T-A, B/R ratios were higher on the outer shelf/slope than on the inner shelf, especially surface B/R ratios were close to or greater than 3.0 on the outer shelf/slope. It seems that picoprocarvates dominated on T-B and the outer shelf/slope of T-A, while this was not the case for T-C and the inner shelf of T-A (Stramski and Morel, 1990; Partensky et al., 1993; Moore et

al., 1995), where the impact of Zhujiang River plume and coastal water might be severe. Another evidence was bathochromic shifts phenomena especially for *Prochlorococcus*. Bathochromic shifts from 440 nm were observed in the entire water column of T-B and on the outer shelf of T-A in November (Fig. 11a). Such a shift to the longer wavelength increased in intensity from 4–6 nm to 40 nm in the deeper water while approaching the slope (Fig. 11b). Bathochromic shifts of ~ 7 nm, consistent with the presence of *Prochlorococcus*, were found in the deep layer of the Sargasso Sea (Bricaud and Stramski, 1990). A similarly strong shift of ~ 40 nm has been observed in the tropical North Atlantic (Lazzara et al., 1996). The shifts we encountered in November strongly suggested the presence of *Prochlorococcus* in this season. This is partly supported by a parallel study of phytoplankton community structure on T-A based on HPLC pigment analysis (Chen et al., 2006). It was revealed that diatom dominated in the Zhujiang River Estuary and

the adjacent coastal area. However, Prymnesiophyta, cyanobacteria and *Prochlorococcus* were main groups in the offshore water. The contribution of cyanobac-

teria and *Prochlorococcus* to chl *a* was 16%–33% and 14%–26% respectively on the outer shelf (Sta. 5 was marked as SCS04 in Chen et al., 2006).

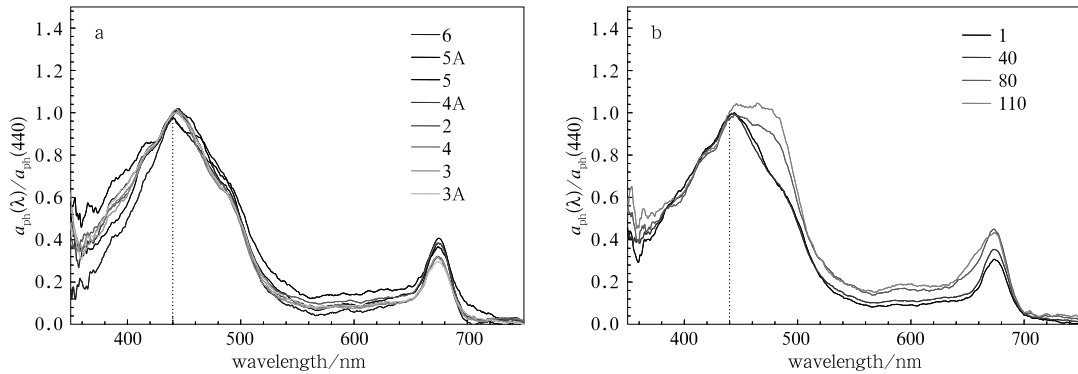


Fig.11. a_{ph} normalized at 440 nm in November 2002. a. Surface distribution on Transect A; b. Vertical distribution at Sta. 3A. The legend in (b) shows the sampling depths in meters. The dotted vertical line in the graphs highlights the normal absorption peak at 440 nm.

3.2 Variations in the absorption spectral model parameters

Among the SEADAS list of MODIS Level 3 products, there are absorption and backscatter coefficients derived from Carder et al. (1999) and QAA (Lee et al., 2002). Carder et al. (1999) chose a hyperbolic tangent function to model the relationship between $a_{ph}(\lambda)$ versus $a_{ph}(675)$ for high-light subtropical regimes as follows:

$$a_{ph}(\lambda) = a_0 \times \exp(a_1 \times \tanh(a_2 \times \ln(a_{ph}(675)/a_3))) \times a_{ph}(675).$$

Table 2 shows the NSCS regional tuning results of the Carder model for the MODIS wave bands centered at $\lambda=412, 443, 488, 510, 531$ and 551 nm. Parameters a_2 and a_3 were set to the same constant values proposed by Carder et al. (1999). Since a_0 is the lead parameter which is directly proportional to $a_{ph}(\lambda)$, hereafter we focused on comparisons of a_0 .

For T-A, a_0 was slightly higher in May 2001 than in November 2002 (Table 2). It was likely due to less pigment package effect arisen from the fact that there were relatively abundant small-size picocaryotes in May. However, variations of a_0 at most of the bands were <10% except at 551 nm. The change of a_0 at 551 nm between two months was ~30%.

Differences of the model parameters between the coastal transect T-C and the shelf transects T-A and T-B in November 2002 were relatively significant (Table 2). A general distribution pattern of a_0 is T-B>T-

A>T-C. For the three bands 412, 443 and 488 nm, a_0 was about 17%–30% lower on T-C than on T-A and T-B. As mentioned above (section 3.1.3), picocaryotes was dominant on T-B and the outer shelf/slope of T-A but not on T-C and the inner shelf of T-A. It was not surprising to find the lowest values of a_0 on T-C, where the pigment package effect was strong due to the minor proportion of picocaryotes.

It appears that the model parameters showed insignificant variation between the two months than between transects, most probably due to the more distinct variation of phytoplankton size structures between the nearshore waters and the outer shelf waters. It is thus suggested that a regional tuning (i.e., from the coastal water adjacent to the ZRE to the NSCS shelf water) may be important for semi-analytical model parameterization. Tuning between the two seasons under study seems less important although a full seasonal cycle of the absorption spectral model is desirable. In addition, the parameters in this region appeared deviated from those originally proposed in Carder et al. (1999) (Table 2), further demonstrating that a single set of parameterization is not applicable globally, and regional tuning is often required.

4 Summary

Variability of the phytoplankton absorption coefficients (a_{ph}) in the northern South China Sea (NSCS) adjacent to the Zhujiang River Estuary (ZRE) was

examined based upon two cruise surveys (May 2001 and November 2002). As expected, significant temporal and spatial variations of $a_{\text{ph}}(675)$ have been found. Short-term variability in May 2001 revealed the impact of heavy precipitation on phytoplankton dynamics downstream of a large river plume induced by heavy precipitation. Temporal differences indicated the deeper mixing in November 2002 due to the stronger winter monsoon. Because $a_{\text{ph}}(675)$ is highly correlated with chl *a*, these variations of $a_{\text{ph}}(675)$ are expected to reflect the pattern of chl *a*, knowledge of which is still rather limited in this region. Furthermore, variations in the absorption characteristics, such as blue/red (*B/R*) ratio and bathochromic shift, inferred change of phytoplankton community structure. For example, picoprocaryotes were probably an important component of the phytoplankton community on the outer shelf/slope of T-A in November, while this seemed not the case for its inner shelf portion, where the impact of Zhujiang River plume and coastal water was high. The results here show the potential of applying a_{ph} , a parameter relatively easy to determine, to obtain valuable information about the phytoplankton standing stock and community structure. In addition, fitting the measured data to the spectral model of a_{ph} of Carder et al. (1999) found greater spatial variations than temporal variations in the model parameters, suggesting that separate models or parameters for coastal and shelf waters are required in order to accurately derive a_{ph} remotely for developing local semi-analytical algorithms.

The NSCS is a complex water body subject to local river plumes and coastal waters modulated by monsoon and other factors. Therefore, the limited data obtained from the two cruises are insufficient to provide a complete evaluation of temporal (event to non-event, seasonal) and spatial (shelf to slope) variability of a_{ph} in this water, and more intensive investigation is required. Nevertheless, our results provide for the first time a preliminary sketch of the spatial and temporal variations of a_{ph} associated with physical processes in this region and the potential for using a_{ph} to imply the variation of phytoplankton community structure.

Acknowledgements

The QuikSCAT wind data were obtained from the Physical Oceanography Distributed Active Archive Center (PO.DAAC) at the NASA Jet Propulsion Laboratory, Pasadena, CA (<http://podaac.jpl.nasa.gov>). We thank Dr. Chuanmin Hu of the South Florida University for his detailed and constructive

comments and suggestions. We are grateful to the crew of the R/V Yanping II, Mr. Chen Zhaozhang and Mr. Chen Dewen for collecting the hydrographic data and processing wind stress data. We also thank Professor John Hodgkiss for editing the manuscript.

References

- Babin M, Stramski D, Ferrari G M, et al. 2003. Variations in the light absorption coefficients of phytoplankton, nonalgal particles, and dissolved organic matter in coastal waters around Europe. *Journal of Geophysical Research*, 108(C7), 3211, doi: 10.1029/2001JC000882
- Bidigare R R, Ondrusek M E, Morrow J H, et al. 1990. In vivo absorption properties of algal pigments. *Proceedings of SPIE*, 1302: 290–302
- Bidigare R R, Smith R C, Baker K S, et al. 1987. Oceanic primary production estimates from measurements of spectral irradiance and pigment concentrations. *Global Biogeochemical Cycles*, 1: 171–186
- Bricaud A, Stamski D. 1990. Spectral absorption coefficients of living phytoplankton and nonalgal biogenous matter: A comparison between the Peru upwelling area and the Sargasso Sea. *Limnology and Oceanography*, 35(3): 562–582
- Bukata R P, Jerome J H, Kondratyev K Y, et al. 1995. Optical properties and remote sensing of inland and coastal waters. CRC Press, Boca Raton, FL
- Cai Weijun, Dai Minhan. 2004. Comment on “Enhanced open ocean storage of CO₂ from shelf sea pumping”. *Science*, 306: 1477C
- Cao Wenxi, Yang Yuezhong, Xu Xiaoqiang, et al. 2003. Regional patterns of particulate spectral absorption in the Pearl River estuary. *Chinese Science Bulletin*, 48(21): 2344–2351
- Cao Wenxi, Yang Yuezhong, Liu Sheng, et al. 2005. Spectral absorption coefficients of phytoplankton in relation to chlorophyll *a* and remote sensing reflectance in coastal waters of southern China. *Progress in Natural Science*, 15(4): 342–350
- Carder K L, Chen F R, Lee Z P, et al. 1999. Semi-analytic Moderate-Resolution Imaging Spectrometer algorithms for chlorophyll and absorption with bio-optical domains based on nitrate-depletion temperatures. *Journal of Geophysical Research*, 104: 5403–5421
- Chen Jixin, Huang Bangqin, Liu Yuan, et al. 2006. Phytoplankton community structure in the transects across East China Sea and Northern South China Sea determined by analysis of HPLC photosynthetic pigment signatures. *Advances in Earth Science (in Chinese)*, 21(7): 738–746

- Chisholm S W, Olson R J, Zettler E R, et al. 1988. A novel free-living prochlorophyte abundant in the oceanic euphotic zone. *Nature*, 334: 340–343
- Cleveland J S. 1995. Regional models for phytoplankton absorption as a function of chlorophyll a concentration. *Journal of Geophysical Research*, 100(C7): 13333–13344
- Cleveland J S, Perry M J, Kiefer D A, et al. 1989. Maximal quantum yield of photosynthesis in the northwestern Sargasso Sea. *Journal of Marine Research*, 47: 869–886
- Cleveland J S, Weidemann A D. 1993. Quantifying absorption by aquatic particles: A multiple scattering correction for glass-fiber filters. *Limnology and Oceanography*, 38: 1321–1327
- Dai Minhan, Zhai Weidong, Cai Weijun, et al. 2008. Effects of an estuarine plume-associated bloom on the carbonate system in the lower reaches of the Zhujiang River estuary and the coastal zone of the northern South China Sea. *Continental Shelf Research*, 28: 1416–1423
- Huang Bangqin, Lin Xueju, Liu Yuan, et al. 2002. Ecological study of picoplankton in northern South China Sea. *Chinese Journal of Oceanology and Limnology*, 20: 22–32.
- IOCCG. 2000. Remote sensing of ocean colour in coastal, and other optically-complex, waters. In: Sathyendranath S, ed., Report of the International Ocean Color Coordinating Group, No. 3. IOCCG, Dartmouth, Nova Scotia Canada, 140
- Kana T M, Glibert P M, Goericke R, et al. 1988. Zeaxanthin and-carotene in *Synechococcus* WH7803 respond differently to irradiance. *Limnology and Oceanography*, 33(6): 1623–1627
- Lau K M, Wu H T, Yang S. 1998. Hydrologic processes associated with the first transition of the Asian summer monsoon: a pilot satellite study. *Bulletin of the American Meteorological Society*, 79: 1871–1882
- Lazzara L, Bricaud A, Claustre H. 1996. Spectral absorption and fluorescence excitation properties of phytoplanktonic populations at a mesotrophic and an oligotrophic site in the tropical North Atlantic (EUMELI program). *Deep-Sea Research I*, 43(8): 1215–1240
- Lee Chen Y. 2005. Spatial and seasonal variations of nitrate-based new production and primary production in the South China Sea. *Deep-Sea Research I*, 52: 319–340
- Lee Z P, Carder K L, Arnone R. 2002. Deriving inherent optical properties from water color: a multi-band quasi-analytical algorithm for optically deep waters. *Applied Optics*, 41: 5755–5772
- Lee Z P, Carder K L, Steward R G, et al. 1998. An empirical algorithm for light absorption by ocean water based on color. *Journal of Geophysical Research*, 103(C12): 27967–27978
- Li Fengqi, Su Yusong. 2001. Analysis of water masses. Qingdao ocean university press, 375–385
- Liu K K, Chao S Y, Shaw P T, et al. 2002. Monsoon-forced chlorophyll distribution and primary production in the South China Sea: Observations and a numerical study. *Deep-Sea Research I*, 49: 1387–1412
- Lorenzen C J, Downs J N, et al. 1986. The specific absorption coefficients of chlorophyllide a and pheophorbide a in 90% acetone, and comments on the fluorometric determination of chlorophyll and pheopigments. *Limnology and Oceanography*, 31(2): 449–452
- Lohrenz S, Weidemann A D, Tuel M. 2003. Phytoplankton spectral absorption as influenced by community size structure and pigment composition. *J Plankton Res*, 25(1): 35–61
- Lutz V A, Sathyendranath S, Head E J H. 1996. Absorption coefficient of phytoplankton: regional variations in the North Atlantic. *Marine Ecology Progress Series*, 135: 197–213
- Mann K H, Lazier J R N. 1996. Dynamics of marine ecosystems. Blackwell Science, 389.
- Mitchell B G, Bricaud A, Carder K, et al. 2000. Determination of spectral absorption coefficients of particles, dissolved material and phytoplankton for discrete water samples. In: Fargion G S, Mueller J L, McClain C R, eds., *Ocean Optics Protocols for Satellite Ocean Color Sensor Validation, Revision 2*, NASA, Goddard space flight center, Greenbelt, Maryland, 125–153
- Mitchell B G, Kiefer D A. 1988. Chlorophyll a specific absorption and fluorescence excitation spectra for light limited phytoplankton. *Deep-Sea Research*, 35(5), 639–663
- Moore L R, Goericke R, Chisholm S W. 1995. Comparative physiology of *Synechococcus* and *Prochlorococcus*: influence of light and temperature on growth, pigments, fluorescence and absorptive properties. *Marine Ecology Progress Series*, 116: 259–275
- Morel A, Antoine D, Babin M, et al. 1996. Measured and modeled primary production in the northeast Atlantic (EUMELI JOGFS program): the impact of natural variations in the photosynthetic parameters on model predictive skill. *Deep-Sea Research I*, 43(8): 1273–1304
- Ning Xiuren, Chai Fei, Xue Huijie, et al. 2004. Physical-biological oceanographic coupling influencing phytoplankton and primary production in the South China Sea. *Journal of Geophysical Research*, 109, C10005, doi: 10.1029/2004JC002365

- Ning Xiuren, Cai Yuming, Li Guowei, et al. 2003. Photosynthetic picoplankton in the northern South China Sea. *Acta Oceanologica Sinica* (in Chinese), 25(3): 83–97
- Partensky F, Hoepffner N, Li W K W, et al. 1993. Photoacclimation of *Prochlorococcus* sp. (Prochlorophyta) strains isolated from North Atlantic and the Mediterranean Sea. *Plant Physiology*, 101: 285–296
- Preisendorfer R W. 1961. Application of radiative transfer theory to light measurements in the sea. *International Union of Geodesy and Geophysics*, 11–30
- Prieur L, Sathyendranath S. 1981. An optical classification of coastal and oceanic waters based on the specific spectral absorption curves of phytoplankton pigments, dissolved organic matter, and other particulate materials. *Limnology and Oceanography*, 26: 671–689
- Qian Weihong, Zhu Yafen, Kang H S, et al. 2002. Temporal-spatial distribution of seasonal rainfall and circulation in the East Asian monsoon region. *Theoretical and Applied Climatology*, 73: 151–168
- Sosik H M, Mitchell B G. 1991. Absorption, fluorescence and quantum yield for growth in nitrogen-limited *Dunaliella tertiolecta*. *Limnology and Oceanography*, 36: 910–921
- Stramski D, Morel A. 1990. Optical properties of photosynthetic picoplankton in different physiological states as affected by growth irradiance. *Deep-Sea Research*, 37: 245–266
- Stuart V, Sathyendranath S, Platt T, et al. 1998. Pigments and species composition of natural phytoplankton populations: effect on the absorption spectra. *Journal of Plankton Research*, 20: 187–217
- Su Jilan. 2004. Overview of the South China Sea circulation and its influence on the coastal physical oceanography outside the Zhujiang River Estuary. *Continental Shelf Research*, 24: 1745–1760
- Tseng C M, Wong G T F, Lin I I, et al. 2005. A unique seasonal pattern in phytoplankton biomass in low-latitude waters in the South China Sea. *Geophysical Research Letters*, 32, LXXXXX, doi:10.1029/2004GL022111
- Wang Guifen, Cao Wenxi, Xu Dazhi, et al. 2005. Variations in specific absorption coefficients of phytoplankton in northern South China Sea. *Journal of tropical oceanography* (in Chinese), 24(5): 1–10
- Wang Gguifen, Cao Wenxi, Xu Dazhi, et al. 2007. Variability of phytoplankton absorption in the northern South China Sea: influence of the size structure and pigment composition of algal populations. *Acta Oceanologica Sinica*, 26(2): 12–25
- Xu Xiaoqiang, Cao Wenxi, Yang Yuezhong. 2004. Relationships between spectral absorption coefficient of particulates and salinity and chlorophyll a concentration in Zhujiang river mouth. *Journal of Tropical Oceanography* (in Chinese), 23(5): 63–71
- Zhai Weidong, Dai Minhan, Cai Weijun, et al. 2005. The partial pressure of carbon dioxide and air-sea fluxes in the northern South China Sea in spring, summer and autumn. *Marine Chemistry*, 96: 87–97
- Zhu Genhai, Ning Niuren, Cai Yuming, et al. 2003. Studies on species composition and abundance distribution of phytoplankton in the South China Sea. *Acta Oceanologica Sinica* (in Chinese), 25(supp.2): 8–23